2021 43rd Annual International Conference of the
IEEE Engineering in Medicine & Biology Society (EMBC)
Oct 31 - Nov 4, 2021. Virtual Conference

Computational Simulation of Breast Tissue with Lesion Characterized by a Thermal Gradient Oriented to Anomalies Smaller than 1 cm of Diameter

R.V. Acero M., I. Bazán, A. Ramírez-García.

Abstract— **In this work, the computational simulation of thermal gradients related to internal lesions according to the phenomenon of pathological angiogenesis is proposed, this is based on the finite element method, and using a three-dimensional geometric model adjusted to suit the real female anatomy. The simulation of the thermal distribution was based on the bioheating equation; it was carried out using the COMSOL Multiphysics® software. As a result, the simulation of both internal and superficial thermal distributions associated to lesions smaller than 1 cm and located inside the simulated breast tissue were obtained. An increase in temperature on the surface of the breast of 0.1 ° C was observed for a lesion of 5 mm in diameter and 15 mm in deep. A qualitative validation of the model was carried out by contrasting the simulation of anomalies of 10 mm in diameter at different depths (10, 15 and 20 mm) proposed in the literature, with the simulation of the model proposed here, obtaining the same behavior for the three cases.**

Clinical Relevance— **The 3D computational tool adjusted to suit the anatomy of the real female breast allows obtaining the temperature distribution inside and on the surface of the tissue in healthy cases and with abnormalities associated with temperature elevations. It is an important characteristic of the model when the behavior of the parameters inside the tissue needs to be analyzed.**

I. Introduction

The development of tools that allow the early detection of anomalies in breast tissue has taken on great importance in recent years. According to the hypothesis proposed by Folkman [1], which indicates a dependence between tumor growth and angiogenesis, no solid tumor can grow above 2 mm without adequate vascular supply. Gautherie [2] observed an increase in temperature and greater blood flow when it comes to tumor tissue, which can be seen reflected in the surface temperature according to Chanmugam [3].

These temperature profiles can be measured by various detection instruments; however, their diagnostic capacity is limited. In response, certain authors [3]–[9] use numerical simulation, based on mathematical model [10], as an additional tool to these instruments to improve sensitivity and fully understand the effect of breast lesions on surface temperature.

Despite having advances in the parameters and the implementation of tools such as neural networks and genetic algorithms, the models described in the literature are far from adapting to the anatomy of the breast in a more realistic way, since in these models, it is divided into layers, simplifying the structures of the mammary gland. One of the main interests of the present study is to improve the approximation to real total thermal distributions (internal and superficial) by approaching the anatomical structure by means of a three-dimensional modeling that involves structures such as lobes and milk ducts and to use very specific parameters for each domain, as well as to analyze anomalies smaller than 10 mm in diameter located into the gland structure.

II. Theoretical Framework

A. Angiogenesis and its relation to tumor formation and consequent temperature elevation

Angiogenesis is the process responsible for the elevation of temperatures in regions where a lesion is located, it is reflected in the phenomenon of blood perfusion (W_b) which is expressed in the bioheating equation. Normally it is a strictly regulated phenomenon [11],[12] however, when vascular growth is complete, angiogenesis becomes a pathological process that accompanies the development of neoplastic and non-neoplastic diseases [13]. This process leads to temperature rises in the region where it occurs [2], [14] and it is generally associated with a surface temperature elevation [6].

B. Bioheating Equation

The bioheating equation is a physic-mathematical model that describes the heat transfer phenomena in the biological tissue, in this case, due to angiogenesis associated with certain abnormalities in the breast.

The mathematical model for heat transfer in tissue was proposed by Pennes [10], this is driven by the fact that there is a thermal equilibrium between blood perfusion at the capillary level and the heat generated by metabolism in the tissue, whose expression is shown in Eq. 1.

$$\rho C_P \frac{\partial T}{\partial t} = \nabla(K\nabla T) + W_b \rho_b C_{p,b}(T_a - T) + Q_m + Q_{ext} \quad (1)$$

where ρ is the density of the tissue $[kg/m^3]$, C_P the specific heat of the tissue $[J/kg\ °C]$, $\partial T/\partial t$ the temperature variation over time, ∇ the gradient operator, K thermal conductivity $[W/(m\ °C)]$, T tissue temperature $[°C]$, W_b blood perfusion flow $[ml\ of\ blood/m^3 s]$, ρ_b blood density $[kg/m^3]$, $C_{p,b}$ specific heat of blood $[J/kg\ °C]$, T_a arterial temperature $[°C]$, Q_m is heat generated by metabolic

R.V. Acero M, I. Bazán, A. Ramírez-García, from the Autonomous University of Aguascalientes, Aguascalientes, México (phone: +52 449 910 9264, ext. 9510; e-mail: al196037@edu.uaa.mx, ivonne.bazan@edu.uaa.mx, alfredo.ramirez@edu.uaa.mx).

activity $[W/m^3]$, and Q_{ext} energy from an external source $[W/m^3]$.

C. Finite Element Method

The finite element method starts from modeling a system to obtain information about its behavior. It begins by subdividing the domain into simple elements which are delimited by points or nodes and each of them has a set of shape functions. Each shape function is associated with certain degrees of freedom (according to dimension). Subsequently, the element stiffness matrix and the load vector are obtained. Once this is done, the global stiffness matrix and the load vector are assembled, boundary conditions are established, and the partial differential equations (PDE) are solved for each element. The solution field is constructed by interpolation of the solution vector and the set of basic shape functions in all elements [15].

The model of the female breast considered was taken from Acero [16], it consists of three-dimensional structures defined for each of the domains; fat, gland, and tumor, to which the epidermis and dermis were added as shown in Fig. 1.

In contrast with other works [3]–[8] that divide the model into layers that represent each involved tissue component, the present model resembles in a closer way the anatomical structure of the real female breast, which might allow us to have more realistic results, mainly inside tissue.

The software used for the simulation was COMSOL Multiphysics®. The 3-D model of the breast, Fig. 1, was imported from SolidWorks®.

III. Methodology

A. Simulation properties

The simulation proposed here focuses on tumors of 5, 6, 7 and 8 mm in diameter and 15 mm in depth, located inside the glandular tissue (conducts and lobes).

The properties of the materials (thermal capacity (C_p), thermal conductivity (K) and density (ρ).) and references from they were obtained are shown in Table I.

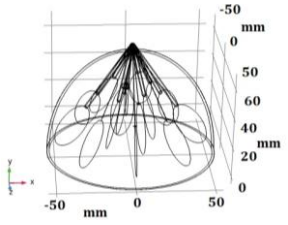

Figure 1. Geometric model of the female breast.

TABLE I. Thermophysical Properties of Materials

Domain	Material Properties			
	$C_p\left[{}^{J}/_{Kg\cdot{}^{\circ}C}\right]$	$K\left[{}^{W}/_{m\cdot{}^{\circ}C}\right]$	$\rho\left[{}^{Kg}/_{m^3}\right]$	$Q_m\left[{}^{W}/_{m^3}\right]$
Fat	2,348 [17]	0.21 [17]	911 [17]	400
Gland	3,475 [8]	0.48 [5]	1,080 [5]	700
Tumor	3,475 [8]	0.48 [5]	1,080 [5]	*VAR*
Dermis	3,475 [8]	0.3140 [8]	1,050 [8]	368.1
Epidermis	3,475[8]	0.2093 [8]	1,050 [8]	0

Regarding physics, the bioheat transfer module was used. It uses the Pennes bioheating equation [10] to model the physical phenomenon. The blood properties (Arterial Temperature (T_a), specific heat ($C_{p,b}$), blood perfusion rate (W_b), blood density (ρ_b) and metabolic heat source (Q_m)), corresponding for each biological tissue involved in the simulation are shown in Table II and have been extracted from Ng and Sudharsan [5], and Chanmugam [3].

TABLE II. Thermophysical Properties of Blood

Domain	Property			
	$T_a\,[^{\circ}C]$	$C_{p,b}\left[{}^{J}/_{kg\,^{\circ}C}\right]$	$W_b\,[{}^{1}/_{s}]$	$\rho_b\left[{}^{kg}/_{m^3}\right]$
Fat	37	4,200	0.0002	1,060
Gland	37	4,200	0.0006	1,060
Tumor	37	4,200	0.012	1,060
Dermis	37	4,200	0.0002	1,200
Epidermis	37	4,200	0	1,200

For all domains, the initial temperature value corresponds to 37 °C. As boundary conditions a fixed temperature for the thoracic wall equal to arterial temperature of 37 °C is assigned and a convective heat flux is added to the upper contour of the dome (epidermis) with a coefficient of heat transfer of 13.5 $[W/m^{2\circ}C]$, and with an environment temperature 20 ° C.

Regarding the mesh, the shape of the element was chosen as tetrahedral, the maximum element size is 3.9 mm, and the minimum element size is 0.167 mm.

B. Model validation

The validation of the model was carried out by means of a qualitative comparison between the model proposed by Chanmugam [3] and the model presented here, both for the simulation of a 10 mm diameter tumor at different depths (10, 15 and 20 mm) with respect to the surface of the dome. In this sense, the thermophysical properties were taken from Chanmugam [3], the initial temperature for all the domains was 37 °C, and the metabolic heat source (Q_m) of the tumor was 5,000 $[W/m^3]$.

As boundary conditions an ambient temperature of 21 ° C is taken, with a heat transfer coefficient of 10 $[W/m^2]$ in the domain of the epidermis, the temperature of the thoracic wall is adjusted to the body core 37 °C.

For the validation case the mesh elements have a tetrahedral shape with a maximum size of 6.13 mm and a minimum size of 0.446 mm, it has a total of 3,508,961 elements. The stationary study was conducted, and the results are shown in the next section.

C. Case study: Variable Q_m

The value of the metabolic heat source (Q_m) for the tumor can vary according to its diameter. The values used for each case were taken from Saniei [7], 5 cases with diameters of 5, 6, 7 and 8 were considered together with the healthy case, takin the Q_m values as 120,800 W/m^3, 60,830 W/m^3, 58,930 W/m^3, 68,450 W/m^3 and 0 W/m^3, respectively. The study was conducted in steady state and the results are shown in the next section.

IV. Results

A. Results of the Validation

Fig. 2 shows the temperature difference on the surface for a tumor with a radius of 5 mm and depths of 10, 15 and 20 mm, this along the arc of the model circumference, where the zero corresponds to the highest point of the dome that represent the breast.

In contrast to Chanmugam [3], who reports a temperature difference of just under 0.6 ° C for a tumor 10 mm deep, here a difference of 0.93 ° C is reported. While for a depth of 15 and 20 mm, Chanmugam [3] reports 0.2 ° C and just under 0.1 ° C, and here 0.3 ° C and 0.2 ° C are obtained, respectively.

Fig. 3 shows the temperature distribution on the surface for a tumor of 10 mm in diameter, with a polar angle of 30° at a depth of 15 mm, which is located within a milk duct, thus simulating a ductal cancer. The increase in surface temperature is 0.3 ° C compared to healthy tissue, which can be seen in the region where the tumor is located.

B. Results of the Case of study: Variable Q_m

Table III shows values of the temperature difference (ΔT), at different depths into the tissue, between healthy case and case with a tumor mass. A vertical cut line is drawn parallel to the "y" axis that crosses all the domains from the thoracic wall to the surface of the breast, where the first column from left to right corresponds to the limit between fat and the lobe in which the tumor is located (A), the second column corresponds to the limit between the lobe and the tumor (B), the third column indicates the limit between the tumor and the fat (C), and finally the last column indicates the temperature values on the surface (D). All these points are fixed positions independently of tumor size except the point B that changes according to it.

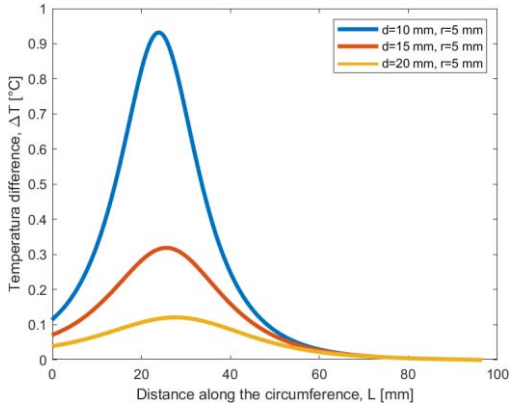

Figure 2. Surface temperature difference (ΔT) for tumor of radius r=5mm and tumor depth of d= 10, d=15, and d=20 mm.

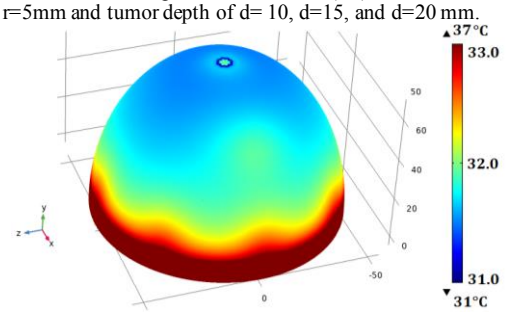

Figure 3. Stages of computer simulation development.

TABLE III. Temperature differences (ΔT) at different depths into the tissue between healthy and tumoral cases (tumor mass located at 15 mm of depth in all cases).

Tumor Size	(A)	(B)	(C)	(D)
5 mm	$0.07\,°C$	$1.19\,°C$	$1.75\,°C$	$0.1\,°C$
6 mm	$0.08\,°C$	$1.17\,°C$	$1.76\,°C$	$0.11\,°C$
7 mm	$0.12\,°C$	$1.34\,°C$	$2.04\,°C$	$0.15\,°C$
8 mm	$0.18\,°C$	$1.57\,°C$	$2.38\,°C$	$0.2\,°C$

It is observed that the temperatures in the tissue interface (C) varies approximately in a range of 1.75 to 2.38 °C, these variations being greater than those that exist at the tissue interface (B), where the range goes from 1.17 to 1.57 °C. A surface temperature variation of 0.1 °C is also observed for a 5 mm tumor and 0.2 °C for an 8 mm tumor. A temperature decrease in the tissue interface (B) between the cases of 5 mm and 6 mm tumor size is observed however keep in mind that this particular interface is not a fixed point in all cases, but it depends on the tumor size and for this reason the temperature reference taken form the healthy case does not correspond to the same position.

The temperature distribution on the surface, from an anterior view, for a healthy case and for a case with a tumor measuring 5 mm, 6 mm, 7 mm, and 8 mm in diameter at a depth of 15 mm is shown in Fig. 4.

V. Discussions

Regard validation, in Fig. 2 we can see the temperature difference on the surface for depths of 10, 15 and 20 mm. The results showed a temperature difference of 0.3 ° C corresponding to 10 mm of depth with respect to that reported by Chanmugam [3], while for 15 and 20 mm of depth they remain within the same range. This is due to the geometry of the model and the domains that the tumor encompasses, where for a 10 mm deep tumor, in the model proposed here, it is still the domain of fat, while for the layered model it is fat and gland.

In Fig. 3, an increase in surface temperature around 32 to 32.2 °C is reported, while Chanmugam [3] reports approximately 32 to 32.4 °C. Results obtained with both models are similar, however, the model here proposed obtains information not only from the surface (as the layered model), but also from the internal structure of the breast.

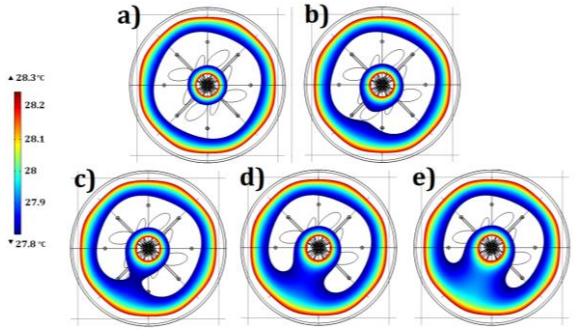

Figure 4. Temperature distribution on the surface. a) healthy case, b) 5 mm tumor case, c) 6 mm tumor case, d) 7mm tumor case, and e) 8 mm tumor case. *The white regions correspond to spaces with temperature out of range, this to highlight the thermal regions on the surface.

About the Case of study: Variable Q_m, in Table III, in the first column from left to right, which corresponds to the boundary between the domains of fat and lobe, we can observe the temperature differences (ΔTs) behavior such that the larger the tumor, the higher the temperature at this point, which allow us to point out that when there is a tumor within the lobe, the temperature of this lobe increases proportionally to the tumor size, presenting small temperature increments approximately of 0.07°C for the smallest tumor (with a diameter of 5mm). In the second and third columns of Table III, which correspond to boundaries of the tumor mass, there were ΔTs of more than 1 °C for all cases, the highest values listed in the table. Nevertheless, in the third column, which corresponds to the boundary between the domain of the tumor and the fat, the values of ΔT were greater than the values presented in the second column (corresponding to boundary between tumor and lobe), therefore, it suggests that there is a greater heat transfer at the limit of the tumor with the fat than with the lobe. Finally, the fourth column shows the ΔTs of the surface of the breast, where an increase of 0.1 °C can be observed for a tumor of 5 mm in diameter and 0.2 °C for one of 8 mm in diameter. This indicates a superficial temperature differences (ΔTs) proportional with tumor size, which matches with results found in other works [3]–[8] focused to obtain superficial temperature patterns.

In Fig. 4 we can see the temperature distribution on the surface for a healthy case and the cases with a tumor of 5, 6, 7 and 8 mm in diameter, where the temperature pattern for the first of them is completely geometric while for the cases with anomaly, an increase in temperature that tends towards the quadrant where the tumor is located was detected. The superficial region affected by temperature increment is larger for tumors with bigger size.

VI. Conclusions

The study of the anatomy and physiology of some processes of the mammary gland, together with the research of previous works, allowed us to select a basic anatomical model, which was simulated with the help of the study of physics and its physiological aspects, thus developing a 3-D computational model that simulates both the anatomy and the bioheating processes associated with pathologies, obtaining realistic results in both: at surface and inside breast tissue.

Anomalies smaller than 1 cm in diameter were analyzed, where an 8 mm diameter tumor can increase the temperature on the breast surface by up to 0.2 °C while a 5 mm one generates a 0.1 °C increase, obtaining its patterns of temperature on the surface which allows us to analyze the temperature increases in the quadrant where the anomaly is located. The model was validated by simulating a tumor of 10 mm in diameter at different depths (10, 15 and 20 mm) taking the Chanmugam [3] data for these cases, obtaining a similar behavior on superficial temperature patterns as a result.

Aknowledgement

We thank the National Council of Science and Technology (CONACYT) for the support granted to carry out this research work and the Autonomous University of Aguascalientes for the financing granted for the development of project PII20-4.

References

[1] J. Folkman, "Tumor Angiogenesis: Therapeutic Implications," *N. Engl. J. Med.*, vol. 285, no. 21, pp. 1182–1186, 1971, doi: 10.1056/NEJM197111182852108.

[2] M. Gautherie, "Thermopathology of Breast Cancer: Measurement and Analysis of in Vivo Temperature and Blood Flow," *Ann. N. Y. Acad. Sci.*, vol. 335, no. 1, pp. 383–415, Mar. 1980, doi: 10.1111/j.1749-6632.1980.tb50764.x.

[3] A. Chanmugam, R. Hatwar, and C. Herman, "Thermal analysis of cancerous breast model.," *Int. Mech. Eng. Congr. Expo. [proceedings]. Int. Mech. Eng. Congr. Expo.*, vol. 2012, pp. 134–143, 2012, doi: 10.1115/IMECE2012-88244.

[4] M. M. Osman and E. M. Afify, "Thermal Modeling of the Normal Woman's Breast," *J. Biomech. Eng.*, vol. 106, no. 2, pp. 123–130, May 1984, doi: 10.1115/1.3138468.

[5] E. Y. K. Ng and N. M. Sudharsan, "An improved three-dimensional direct numerical modelling and thermal analysis of a female breast with tumour," *Proc. Inst. Mech. Eng. Part H J. Eng. Med.*, vol. 215, no. 1, pp. 25–38, 2001, doi: 10.1243/0954411011533508.

[6] J. Kwok and J. Krzyspiak, "Thermal Imaging and Analysis for Breast Tumor Detection," p. 18, 2007.

[7] E. Saniei, S. Setayeshi, M. E. Akbari, and M. Navid, "Parameter estimation of breast tumour using dynamic neural network from thermal pattern," *J. Adv. Res.*, vol. 7, no. 6, pp. 1045–1055, 2016, doi: https://doi.org/10.1016/j.jare.2016.05.005.

[8] S. Shrestha, G. Kc, and D. Gurung, "Transient Bioheat Equation in Breast Tissue: Effect of Tumor Size and Location," 2020, doi: 10.22606/jaam.2020.51002.

[9] A. Lozano, J. C. Hayes, L. M. Compton, J. Azarnoosh, and F. Hassanipour, "Determining the thermal characteristics of breast cancer based on high-resolution infrared imaging, 3D breast scans, and magnetic resonance imaging," *Sci. Rep.*, vol. 10, no. 1, p. 10105, 2020, doi: 10.1038/s41598-020-66926-6.

[10] H. H. Pennes, "Analysis of Tissue and Arterial Blood Temperatures in the Resting Human Forearm," *J. Appl. Physiol.*, vol. 1, no. 2, pp. 93–122, Aug. 1948, doi: 10.1152/jappl.1948.1.2.93.

[11] "Modelos y ensayos para el estudio de la angiogénesis," *Medisan*, vol. 20, no. 1, pp. 100–108, 2016, Accessed: Nov. 13, 2019. [Online]. Available: http://web.a.ebscohost.com.dibpxy.uaa.mx/ehost/pdfviewer/pdfviewer?vid=1&sid=ced462a3-596b-4181-819e-93954e8ca101%40sdc-v-sessmgr01.

[12] P. Khosravi Shahi, A. del Castillo Rueda, and G. Pérez Manga, "Angiogénesis neoplásica ," *Anales de Medicina Interna* , vol. 25. scieloes , pp. 366–369, 2008.

[13] V. S. Socarrás, "Papel de la angiogénesis en el crecimiento tumoral," *Rev. Cuba. Investig. Biomed.*, vol. 20, no. 3, pp. 223–230, 2001, Accessed: Nov. 13, 2019. [Online]. Available: http://web.a.ebscohost.com.dibpxy.uaa.mx/ehost/pdfviewer/pdfviewer?vid=1&sid=c8157159-95fc-4c94-a971-ac5193bc69f4%40sessionmgr4008.

[14] R. Lawson, "Implications of surface temperatures in the diagnosis of breast cancer," *Can. Med. Assoc. J.*, vol. 75, no. 4, p. 309, 1956.

[15] T. R. Chandrupatla, A. D. Belegundu, and J. E. de la Cera Alonso, *Introducci¢n al estudio del elemento finito en ingenier¡a*. Pearson Educación, 1999.

[16] R. V. Acero M., I. Bazán, and A. R. García., "Computational Model of Breast Tissue with a Lesion defined by a Thermal Gradient," *Present. GMEPE/PHACE 2021*, 2020.

[17] Comsol, "Comsol Multiphysics," *User Guid.*, 2012, doi: 10.1016/S0260-8774(99)00111-9.